Schweizerische Eidgenossenschaft
Confédération suisse
Confederazione Svizzera
Confederaziun svizra

Federal Department of the Environment, Transport, Energy and Communications DETEC

Swiss Federal Office of Energy SFOE
Energy Research and Cleantech Division

REEL Demo – Romande Energie ELectric network in local balance Demonstrator

Deliverable: 4b Ageing Analysis of a BESS

Demo site: Chapelle

Developed by
Dr. Dimitri Torregrossa and Julien Furrer,
Aurora’s Grid for Romande Energie

[Lausanne, 08.01.2019]

1. Description of deliverable and goal

1.1. Executive summary

This deliverable shows the impact of some specific operating conditions such as very high value of current, depth of discharge and temperature that could be happens in BESS deployed in smart-grid.
A computation of benefit and ageing associated with a BESS installed in a real house for increasing its renewable energy self-consumption is presented.

1.2. Research question

How it is possible to account for the impact of high current values to the ageing of Li-ions batters energy storage systems (BESS)?

1.3. Novelty of the proposed solutions compared to the state-of-art

In the literature is possible to find some software computing optimal size of the battery storage system for different type of applications. No one of the existing software is accounting for the impact of high value of current, temperature and depth of discharge on the ageing of the battery itself.
It is difficult to find a comprehensive study accounting for all the ageing factors.

1.4. Description

This deliverable highlighted the importance of the ageing phenomena in Li-ions BES, with a specific focus on C-rate, DoD and temperature effects.
After reviewing the main ageing processes and giving computation of capacity fading and increase of equivalent series resistance for each of the above ageing factors, this document illustrates some simulations results associated with the deployment of BES in buildings.
The presence of BES in a building equipped with a PV plant can be, economically speaking, very interesting. Of course, in order to increase as much as possible its profitability, its lifetime has to be extended by an appropriated ageing-management. The results of this document shows that by managing the ageing of the BES it is possible to double its benefit (compared to a not ageing-aware strategy).
Full description of the work is provided on the annex

2. Achievement of deliverable:

2.1. Date

[27-12-2018]

2.2. Demonstration of the deliverable

The software has been tested for a real house located in Neuchatel, since for this house there were available PV production and load consumption for more than one year.

Romande Energie will provide these types of measurements for other buildings located in canton VD thanks to the usage of GridEye monitoring devices.

Romande Energie will deploy the results of this deliverable for sizing two battery systems to be located in Rolle.

3. Impact

This work contributes to the improvement of the BESS management methodologies undertaken in the frame of the WP4, notably for the operation of the battery storage systems for grid control. Future works will be focused on the possibility to provide ancillary services to the grid via distributed LI-ions BES located in buildings, in order to increase, much more, the profitability of BES.

Table of Contents

1 Acronyms 3

2 Introduction 4

3 Effects of charging current 5

3.1 Capacity loss 6

3.2 Resistance increase 7

4 Effects of discharging current 8

4.1 Capacity loss 9

4.2 Resistance increase 11

4.3 Available energy 13

5 Effects of depth of discharge 13

5.1 Capacity loss 14

5.2 Resistance increase 15

6 Effects of storing temperature 17

6.1 Capacity loss 17

6.2 Resistance increase 18

7 Effects of combined cycling at temperature above the normal one 20

7.1 Capacity loss 20

7.2 Resistance increase 22

8 Effects of abusive high temperature test and evaluation of risk of short-circuit and irreversible performance degradations 22

9 Risk of short-circuit in a lithium ion cell 25

10 Evaluation of lifetime of targeted battery pack with the software Aurora's Grid 1.0 27

10.1 Operating conditions 27

10.2 Simulation results 28

11 Conclusions and Perspective.....31

12 References.....32

1 Acronyms

BMS: Battery Management System

BES: Battery Energy Systems

DoD: Depth of Discharge

EoL: End-of-Life

ISC: internal short circuit

LCO: Lithium Cobalt Oxide

LFP: Lithium Iron Phosphate

LMO: Lithium Manganese Oxide

NMC: Lithium Nickel Cobalt Manganese Oxide

SEI: Solid Electrolyte Interphase

SOC: State-of-Charge

2 Introduction

The goal of this document is to provide a comprehensive overview on the ageing phenomena on Lithium-ion battery, with specific focus on the effect of storing temperature, C-rate and depth of discharge.

First, the document analysis the main ageing factors, such as the extracted current, the temperature and the SOC. Then, for each of these ageing factors specific graphs showing the capacity fading and the increase of equivalent series resistance are illustrated. These graphs have been built thanks to a comprehensive state of the art of existing models and available experimental characterizations that have been assembled to obtain an overall computation of the ageing effects.

The ageing computation is focused on the capacity fading, limiting the autonomy of the battery, as well as the equivalent resistance increase, limiting the delivered power.

A specific chapter, is dedicated to the evaluation of the risk of short-circuit in Li-ions cell.

Finally, thanks to an ageing model developed by Aurora's Grid accounting for all the ageing factors, namely C-rate in charging and discharging, middle SOC, temperature and DoD, some simulation have been run. More specifically, a simulated environment of a specific building has been deployed and BES of different sizes have been introduced in these simulations for computing the advantage in terms of increased energy self-consumption.

3 Effects of charging current

Charging and discharging current is one of the main ageing factor in a Li-ion cell.

Figure 1 illustrates schematically the charging process through a Li-ion cell from an electrochemical point of view.

During the charging phase, lithium ions migrates from the cathode to the anode, which has specified intercalation layers in its lattice structure to host the lithium ions reaching its surface. In general, the charging process of a lithium-ion battery is limited by two main factors: oxidation of the electrolyte due to high potentials at the cathode and lithium plating at the anode. Both effects lead to irreversible loss of active material [1].

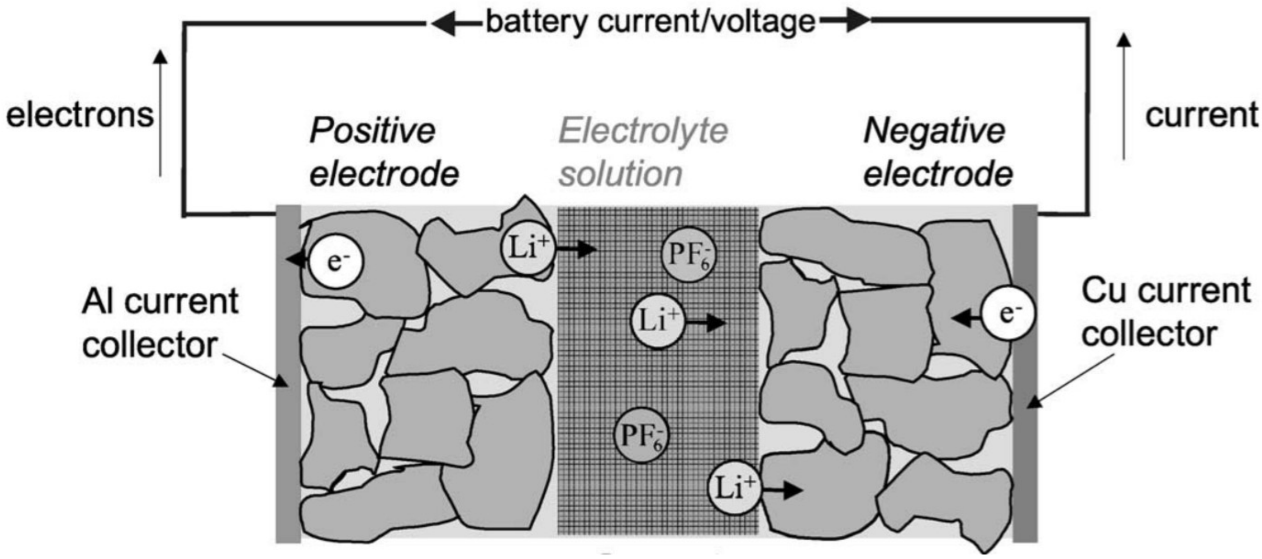

Figure 1: Schematic representation of lithium intercalation during charging of the battery [2].

Lithium plating is the undesired reduction of lithium ions to metal lithium on the anode active surface, taking place instead of the regular intercalation process. The equilibrium potential of lithium intercalation into graphite is only a little higher than the equilibrium potential of the plating reaction, consequently these two phenomena compete each other during the charging phase. Under high charging current, the graphite potential can become lower than the Li/Li^+ potential, leading to the reduction of the Li^+ ions into metallic lithium and its consequent deposition onto the surface of the graphite instead of intercalation. The plated lithium becomes then isolated from the conductive electrode, leading to an irreversible loss of active material. This metallic lithium deposited on the graphite tends to form dendrites, which in the worst case they can keep growing upon cycling until they pierce the separator causing an internal short circuit [3]. On the other hand, the oxidation of the electrolyte occurs at high cathode overpotentials. Overcharging the cell can cause irreversible damages to cathode lattice structure. In fact overpotential increases the heat generation that can accelerate oxidative reactions between the electrolyte and the delithiated cathode [1]. To minimize theses detrimental effects, low charging currents and the respect of the upper voltage limit are recommended [4].

3.1 Capacity loss

Figure 2 illustrates the capacity degradation at performed cycles with three different chemistries and different currents corresponding to 1C, 3C and 5C during the charging phase. The tests were performed at 100% DoD, 25°C and 1C discharge rate. Cell A is a LMO+NMC blend, cell B is a NMC+LCO blend and cell C is LFP. In general, we observe that degradation is faster at higher charging rates. Because of different cycle lifetimes of the chemistries the impact is different, however the trends are similar and allow the generalization of charge rate impact. For example, cell A in Figure 2, at a charging rate of 5C can perform around 55 % less cycles then the same cell cycled with a charging rate of 1C.

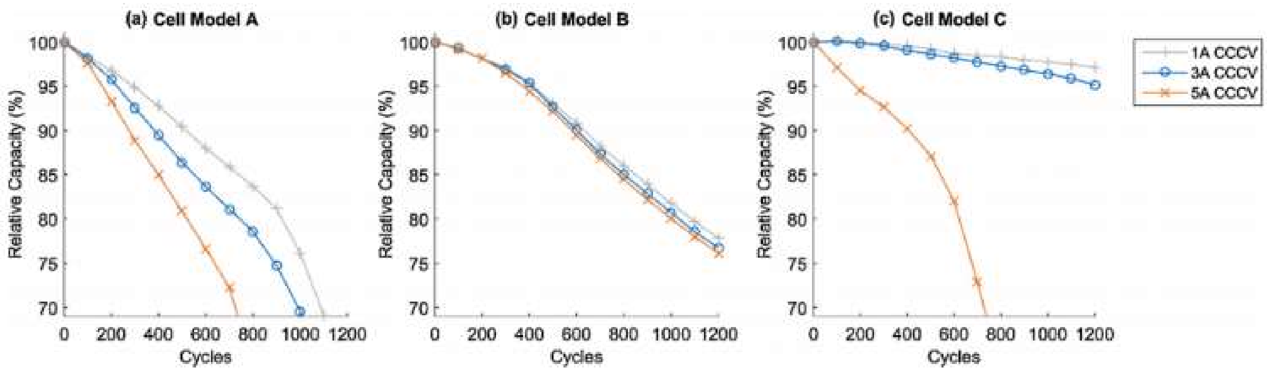

Figure 2: Capacity loss at different charging currents. [1]

In opposition to the previous one, Figure 3 allows the analysis of lower charging rates, namely 0.2C and 0.5C. The tests were performed at 100% DoD, 25°C and a discharge rate of 1C on a NMC lithium-ion battery. The trend is similar to the one observed for larger charging rates, leading to slower degradation of the battery in terms of capacity for lower rates. In this case charging the battery with a rate of 1C instead of 0.2C can reduce the number of cycle to end of life (80% of residual capacity) by more than 80 %.

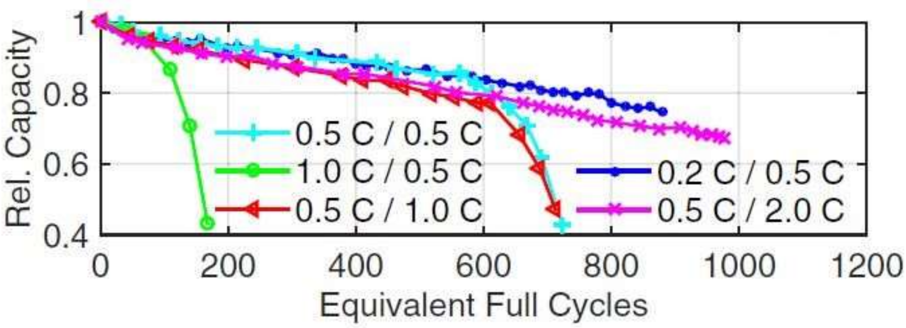

Figure 3: Relative capacity evolution depending on the charging/discharging rate. NMC [5]

The analysis of results obtained from the literature allows the construction of a general mathematical model that emulates the impact of the charge rate on the capacity loss of a NMC battery. This model can later be rescaled to a battery under study according to its specific parameters. Figure 4 shows the evolution of battery capacity along the cycle lifetime considering different charge rates. As presented before, higher charge rates result in faster degradation of the battery. It is important to highlight that the result shown on Figure 4 have been built by Aurora's Grid thanks to its model.

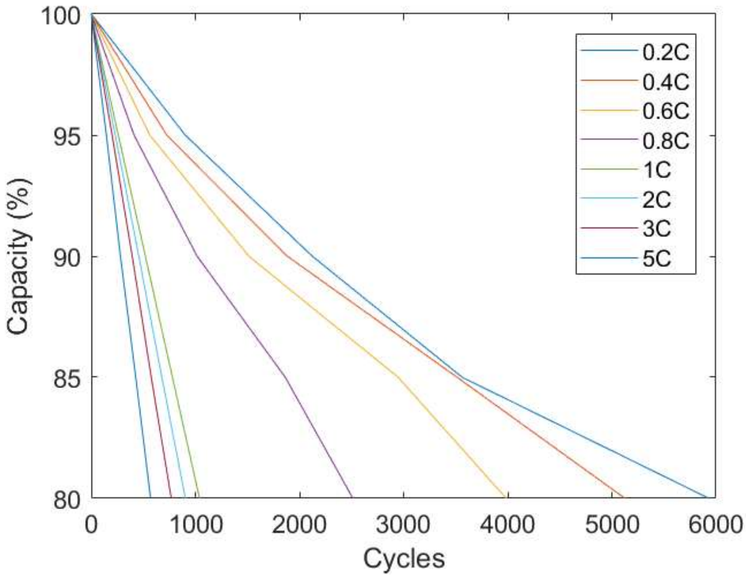

Figure 2: Capacity degradation at different charging rates for a NMC battery [1]

3.2 Resistance increase

Figure 5 illustrates the impact of charge rate on the increase of internal resistance for an NMC battery at 100% DoD, 25°C and 1C discharge rate. The results concern charge rates of 0.2C, 0.5C and 1C. The figure's legend is the same as for Figure 3 and Figure 6. The mechanism is like the one describing the capacity loss of the battery. We can see that when charging the battery at 0.5C

[1] Model developed by Aurora's Grid

instead of 1C, we reach an increment of internal resistance of 40 % after 700 cycles against a 60 % increase after around 175 cycles.

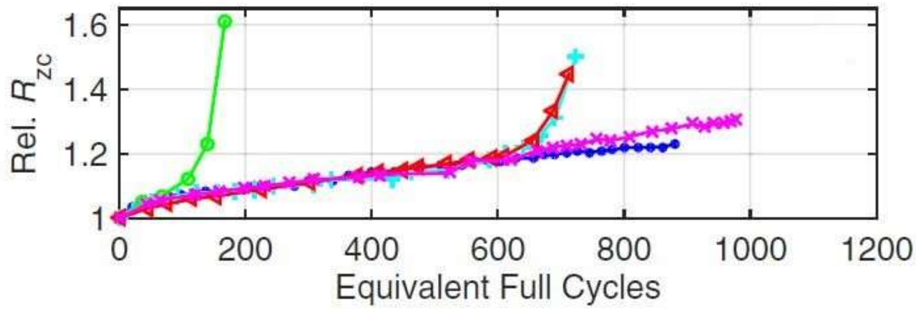

Figure 5: Relative resistance evolution at different charging/discharging rates. NMC [5]

Figure 6 represents the relationship between internal resistance and battery capacity at the same conditions as Figure 5. It seems that the charging rate doesn't have a significant impact on the correlation between resistance increase and relative discharge capacity, except for the fact that, as stated before, the battery degrades faster at higher charging currents.

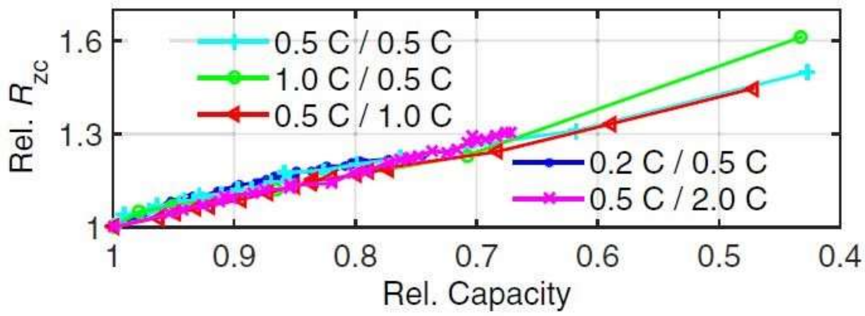

Figure 6: Correlation of relative resistance with the relative capacity at different rates. NMC [5]

4 Effects of discharging current

As for the charging current, a higher discharging rate generally corresponds to an increased ageing of the battery. Within the very first cycle of every battery, a solid electrolyte interphase (SEI) forms on the carbon anode. This layer is the result of electrochemical decomposition of the electrolyte on the electrode surface. It acts as a protective layer because it does not allow the direct contact between the electrode and the electrolyte, hence preventing further reactions, but still allows the passage of the lithium ions. Even if the main formation of the SEI happens in the very first cycles, it keeps growing slowly while cycling. When the battery is cycled under high discharge rate, the internal temperature will rise due to ohmic effect causing the formation of the SEI to proceed at a faster rate. The continuous thickening of the SEI film can reduce the ability of the lithium ions to reach the anode causing an increase in the internal resistance and a capacity degradation of the battery. At elevated current the continuous reaction on the anode can even causing some cracks on its surface, reducing even more the available active material [6]. The SEI growth caused by high discharge rate also cause volume changes, which cause contact loss of active material and modification in porosity of the anode. These last phenomena have the effect to increase the impedance of the cell and reduce the active material available, in other words they lead to power and capacity fade [7].

Normally we cannot decide the value of discharge current since it depends on the specific application. For this reason, it is important to know exactly the current profile deployed during discharging phases in order to evaluate, in the most accurate way, its impact on the cell's lifetime.

4.1 Capacity loss

The discharge rate appears to be an important factor impacting the capacity degradation of a battery. Figure 7 depicts the results for a NMC battery for small rates going from 0.33C up to 3C. The tests were performed at 25°C, 100% DoD and 1C charge rate. The observation of the results indicates that small discharge rates does not have a significant impact, which is confirmed by more detailed analysis. Taking as a reference the cycles performed till reaching the end of life condition, we can see that discharging the battery at 3C versus C/3 reduces its lifetime of around 25 %.

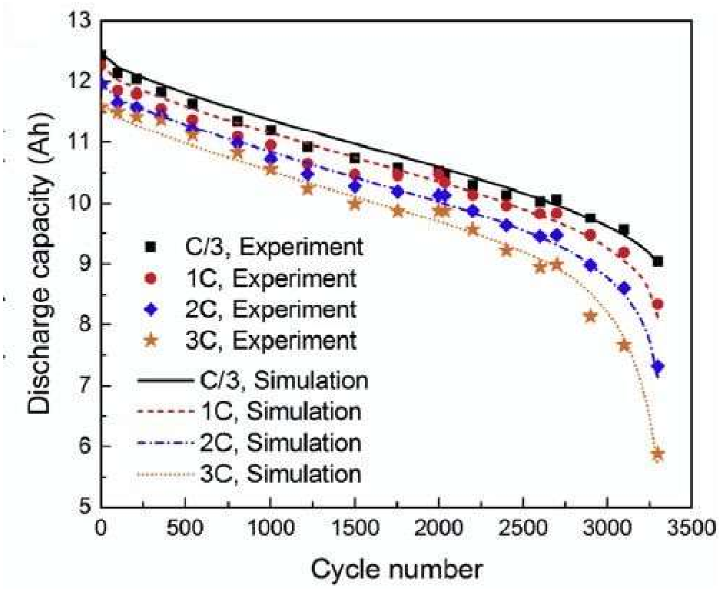

Figure 7: Evolution of cell capacity at different discharge rates. NMC [3]

On the other hand, Figure 8 represents the capacity degradation for large discharge rates for a LFP battery. Namely, the tests were performed at 1C, 5C, 10C and 15C discharge rate with 100% DoD, 25°C and 1C charge rate. It is straightforward that the capacity loss is strongly impacted by the discharge rate when large values are considered. In this case discharging the battery at a rate of 15C instead of 1C, can reduce the lifetime of the battery by more than 80 %.

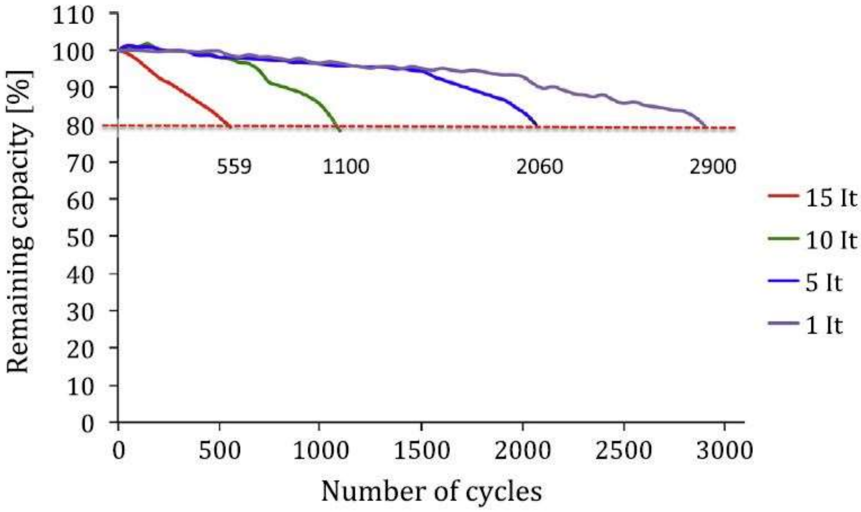

Figure 8: Evolution of remaining capacity at different discharge rates. LFP [8]

The analysis of results presented before, allows the development of a general model simulating the impact of the discharge rate on the capacity degradation along the cycle lifetime of a NMC battery. Results of the model are presented on Figure 9 below. This model can then be rescaled to a battery under study according to its specific parameters. It is important to highlight that the results shown in Figure 9 are not available in the literature and have been built by Aurora's Grid.

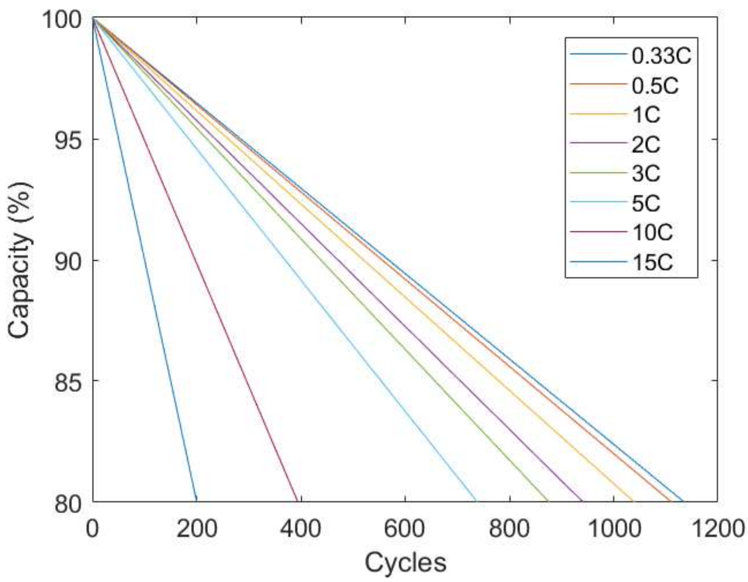

Figure 9: Capacity degradation at different discharging rates for a NMC battery [2]

[2] Model developed by Aurora's Grid

4.2 Resistance increase

Concerning the equivalent series resistance, Figure 10 represents the increase of internal resistance during cycle lifetime for different values of discharge rate: 1C, 5C, 10C and 15C. The tests were performed on an LFP battery at 100% DoD and 25°C. The end value of resistance corresponds to the measurement at capacity End-of-Life of the battery (capacity reaching 80% of its nominal value). As the discharge rate rises, the increase of resistance is more significant. However, it doesn't imply a higher end-value. Indeed, at very high rates, the cycle lifetime is very short, and the resistance doesn't have time to increase, as for the test at 15C. For comparison, the 23 % of resistance increase at end of life for the battery cycled at 1C is reached at 2900 cycles versus only 320 cycles when the battery is discharged at 15C, this means almost 90 % less cycles were performed to reach the same resistance increase.

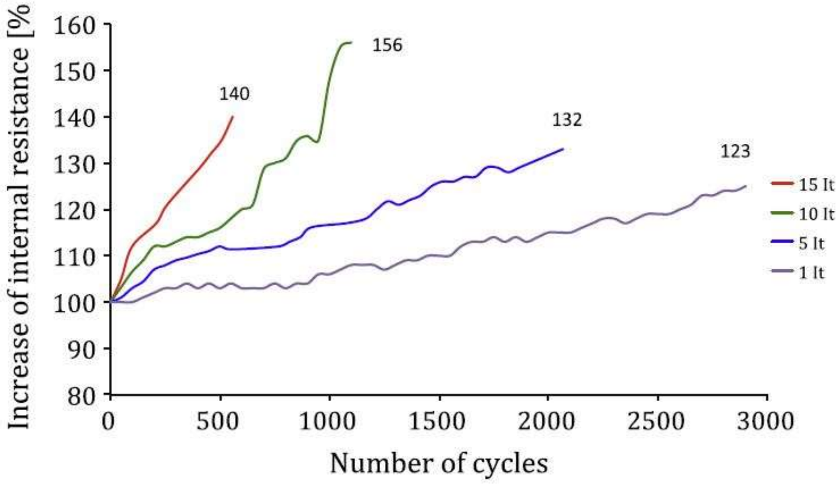

Figure 10: Increase of internal resistance versus cycle life for different discharge rates. LFP [8]

The impact of discharge rate on the increase of internal resistance along the cycle lifetime can be modelized based on available data and is presented on Figure 11. This model can then be rescaled to a battery under study according to its specific parameters.

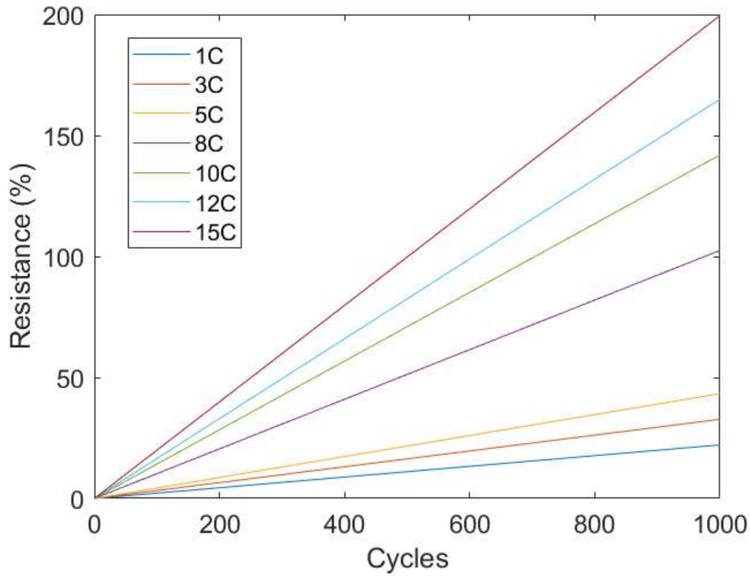

Figure 11: Resistance increase at different discharging rates [3]

Moreover, it is possible to represent the resistance increase as a function of the discharged capacity. On Figure 12, the resistance increase appears to be lower at 15C than at 10C at the EoL conditions (80% of reached capacity). This is due to the fact that the capacity degradation is dominant, and the EoL has been reached in a small number of cycles. It is important to highlight that the results shown in Figure 11 and 12 are not available in the literature and have been built by Aurora's Grid.

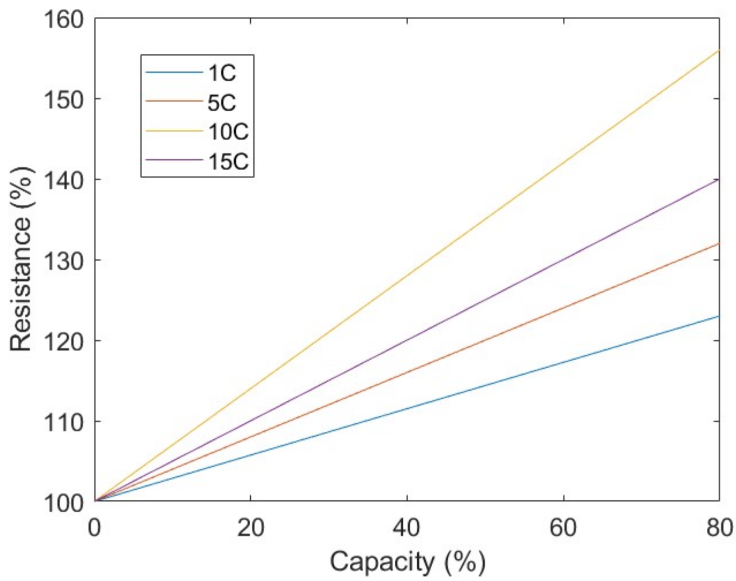

Figure 12: Correlation between resistance increase and capacity degradation [3]

[3] Model developed by Aurora's Grid

4.3 Available energy

In addition to the impact of discharge rate on ageing mechanisms of the battery, it is important to notice its influence on the extractable energy during a cycle. Indeed, at high rates the available energy is considerably reduced due to an increase of internal resistance. This phenomenon is depicted on Figure 13 for the studied battery, LG HD2C 2100mAh 20A. For example, at 15C the discharged energy is 5% lower compared to nominal conditions. Inversely, in order to extract the full stored energy, it is recommended to discharge the battery at low rates, ideally below 1C [8].

However, this topic is relevant mostly for energy applications with low time constants, were the discharge rate can be reduced. In high power applications, such as a frequency control, high currents are necessary while the energy efficiency is not so crucial.

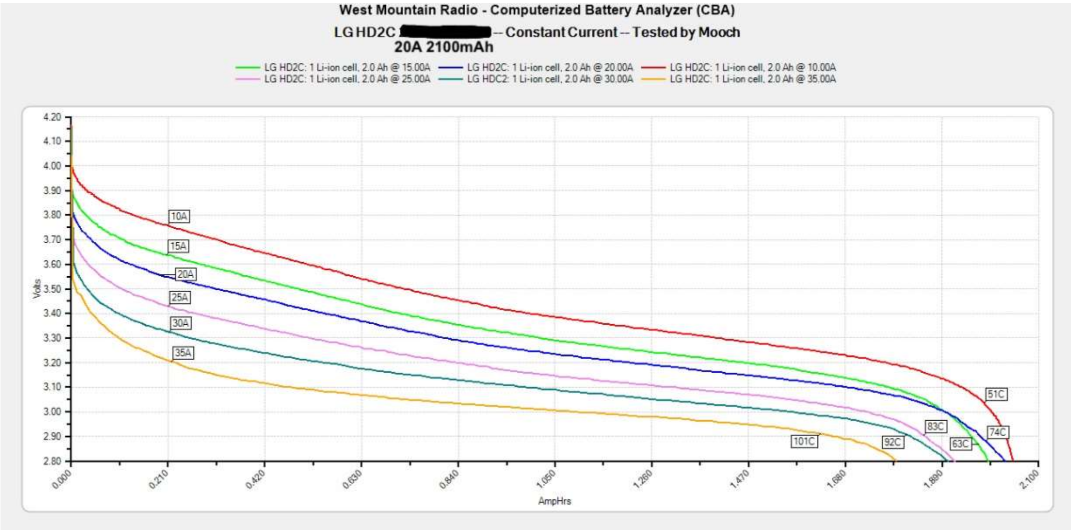

Figure 13: Discharge efficiency at different discharge rates – LG HD2C 18650 2100mAh 20A [9]

5 Effects of depth of discharge

Another important parameter influencing the aging of lithium-ion batteries is the depth of discharge, DoD. The general trend is an increase in capacity degradation when performing deeper cycles. The reason is that cells cycled at higher DoD are subjected to larger load oscillations due to the anode expansion during the lithium intercalation in the graphite. Higher DoD corresponds to a higher expansion of the graphite because more lithium ions reach the anode. This expansion and contraction repeated upon a large number of cycles can cause damages on the surface due to fatigue stress causing loss of active material [10].

5.1 Capacity loss

Figure 14 represents the influence of cycling DoD on the capacity loss of a LFP lithium battery at 25°C and 1C charge/discharge rate. It can be observed that cycles at higher DoD lead to faster capacity degradation. It must also be mentioned that cycling at lower DoD implies also that less energy extracted from the battery in a cycle. We can observe that cycling the battery with a depth of 100 % can reduce its lifetime in terms of cycles up to 75% with respect the same battery cycled at a depth of discharge of only 55%.

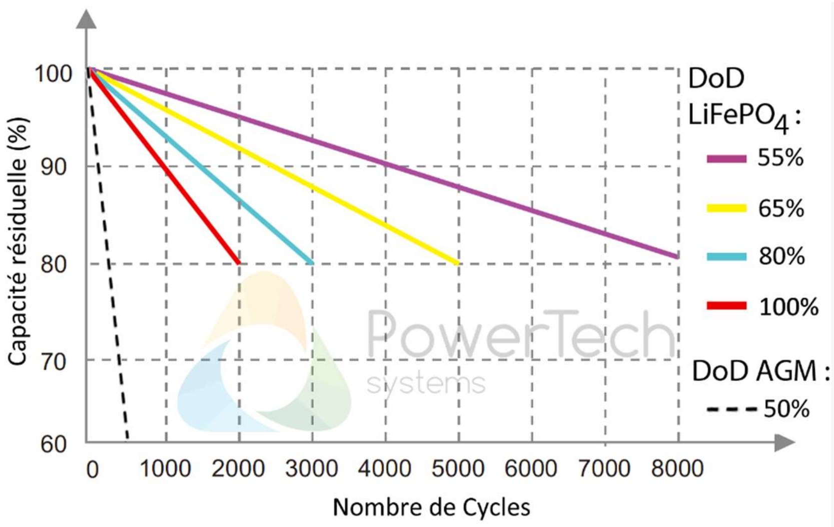

Figure 14: Capacity evolution versus cycle number for different depth of discharge. LFP [11]

The same observation can be made based on modelling results concerning NMC chemistry and represented on Figure 15. This model can then be rescaled to a battery under study according to its specific parameters. It is important to highlight that the results shown in Figure 15 are not available in the literature and have been built by Aurora's Grid.

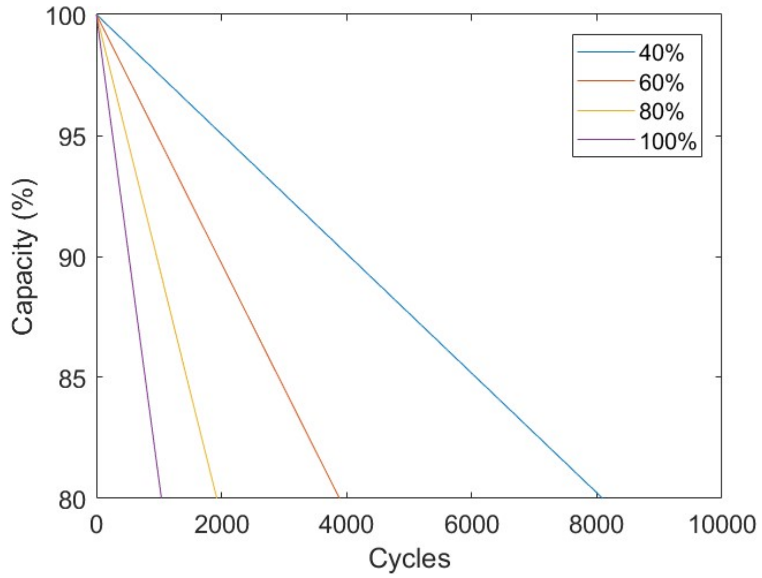

Figure 15: Capacity evolution versus cycles at different DOD. NMC [4]

5.2 Resistance increase

As for the impact of discharge rate, data is available concerning the value of resistance at capacity End-of-Life depending on the cycling DoD for the LFP chemistry. Cycling which higher DoD implies a faster degradation (increase) of the internal resistance of the battery. Whereas, lowering the DoD allows the preservation of the battery resistance. For example, the 19 % of resistance increase reached at end of life after 10000 cycles for a battery cycled at 60 % of DOD, takes only 1550 cycles at 100 % DOD, i.e. a reduction in terms of cycles of around 85 %.

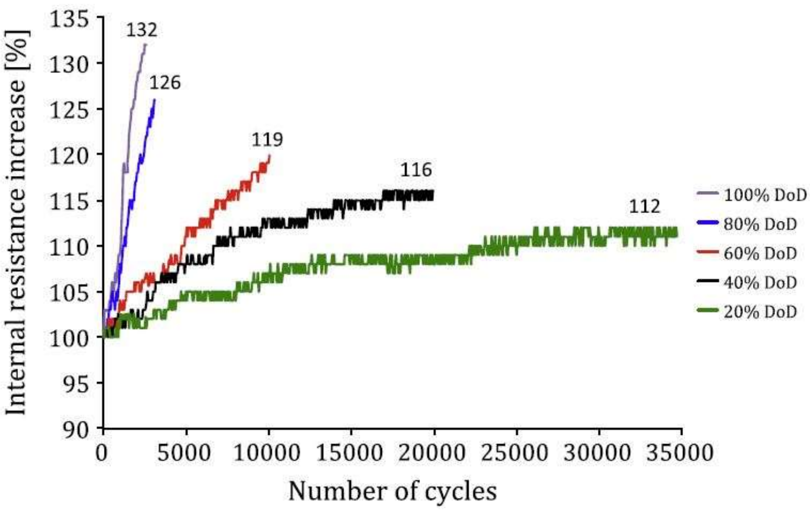

Figure 16: Evolution of internal resistance at different depth of discharge. LFP [8]

[4] Model developed by Aurora's Grid

On the other hand, the same trend can be identified for the NMC chemistry as depicted on Figure 17, where the resistance evoulution is plotted against equivalent full cycles, which means that the number of cycles is normalized by the nominal capacity value. The tests were performed at 35°C and 1C charge/discharge rate. Low DoD of cycling leads to slower increase of the internal resistance, while higher values result in an accelerated degradation. Moreover, DoD between 0% and 20% seem to have a similar impact. Once again we can compare cycling at 100 % DoD and 50 % DoD: the resistance doubles after 30 % less cycles when cycling at higher DoD.

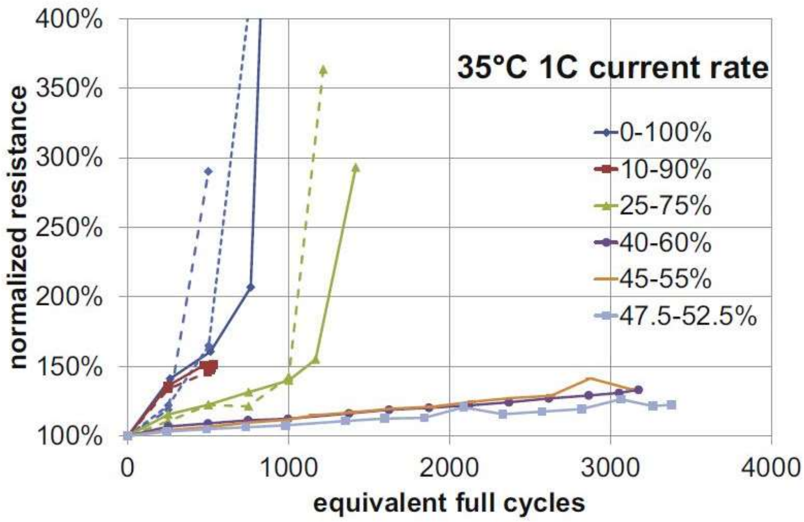

Figure 17: Normalized resistance at different depth of discharge. NMC [12]

The impact of cycle DoD on the resistance increase during lifetime can therefore be modelized based on the analysis of available data. This model can then be rescaled to a battery under study according to its specific parameters. Figure 18 shows the increase of resistance along cycle lifetime at 15C discharge rate for different values of DoD. It is important to highlight that the results shown in Figure 18 are not available in the literature and have been built by Aurora's Grid.

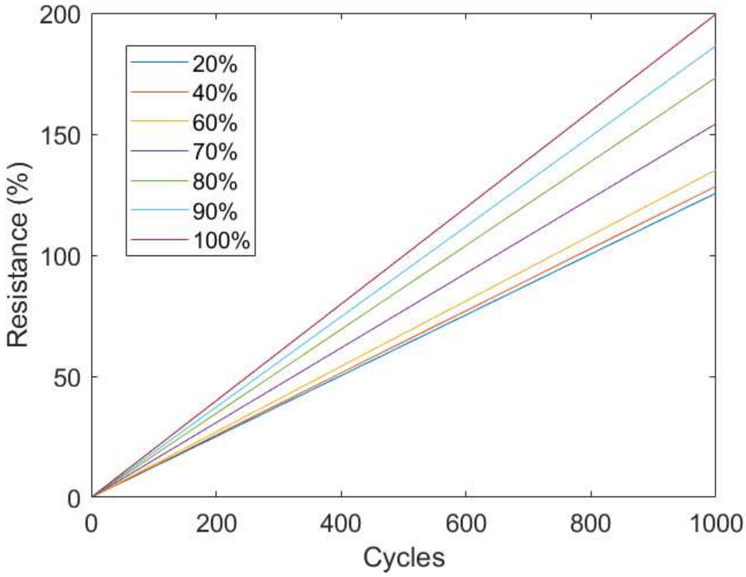

Figure 18: Resistance evolution at different depth of discharge versus cycles [5]

6 Effects of storing temperature

The main effect of a high storage temperature (higher than the nominal one, i.e 25 Celsius degree) is an increase in capacity degradation and internal resistance. Temperature increase facilitates the electrolyte decomposition reaction and the corresponding growth of the SEI. In general the impact of the temperature on capacity fade can be considered as exponential, described by the Arrhenius law for chemical reactions [13]:

$$k = Ae^{-\left(E/_{RT}\right)}$$

Where:

- k is the rate constant of the chemical reaction;
- A is a constant for a given reaction;
- E is the activation energy of the reaction ($J.mol^{-1}$);
- R is the universal gas constant ($J.K^{-1}.mol^{-1}$);
- T is the absolute temperature (K).

In addition to that for lithium battery containing manganese, in a long storage at high temperature (at least over 60°C) manganese dissolution can happen resulting in a loss of cathode active material [14].

6.1 Capacity loss

Calendar ageing describes the capacity loss that occurs in the battery during long storage periods without any charge/discharge. Figure 19 depicts the remaining capacity along the storage period in

[5] Model developed by Aurora's Grid

days for a NMC chemistry with an initial SOC of 50% (battery half charged). The tests were performed at 35°C, 50°C and 65°C and show that higher temperatures lead to an acceleration of the capacity loss. At 35°C, the capacity loss even after 30 weeks (≈ 200 days) is of 5%, while reaching 20% at 65°C for the same storage period.

Similar observation can be made from Figure 20 concerning also the NMC technology, with tests performed at 80% of initial SOC.

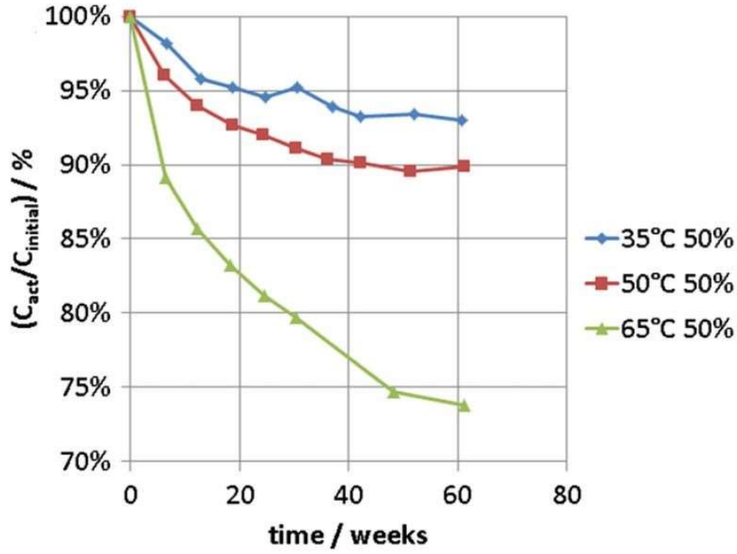

Figure 19: Calendar ageing at different storage temperatures and 50% SOC. NMC [13]

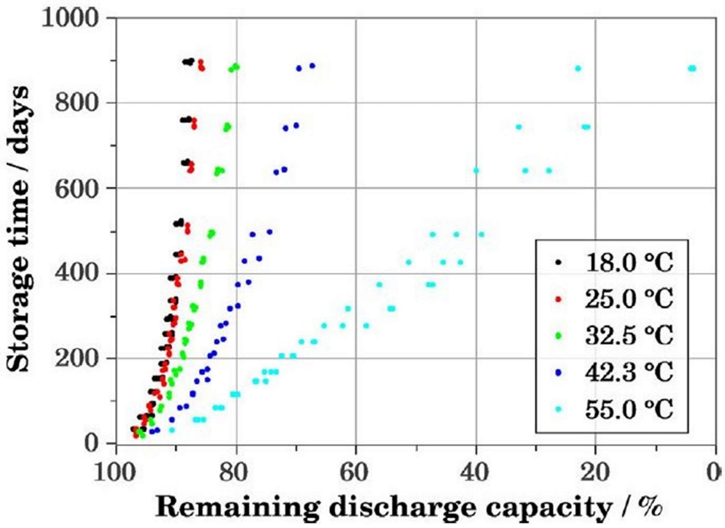

Figure 20: Calendar ageing at different storage temperatures and 80% SOC. NMC [15]

6.2 Resistance increase

Storage impacts not only the capacity of the battery, but also its internal resistance. Figure 21 presents the normalized internal resistance along the storage period in days for a LFP chemistry with an initial SOC of 100% (battery fully charged). The tests were performed at 25°C (cyan curve), 40°C (yellow curve) and 60°C (red curve). It can be observed that storing at room temperature (blue curve at 25°C) does not have a real impact on the resistance. It is only at higher temperatures that the internal resistance increases along time.

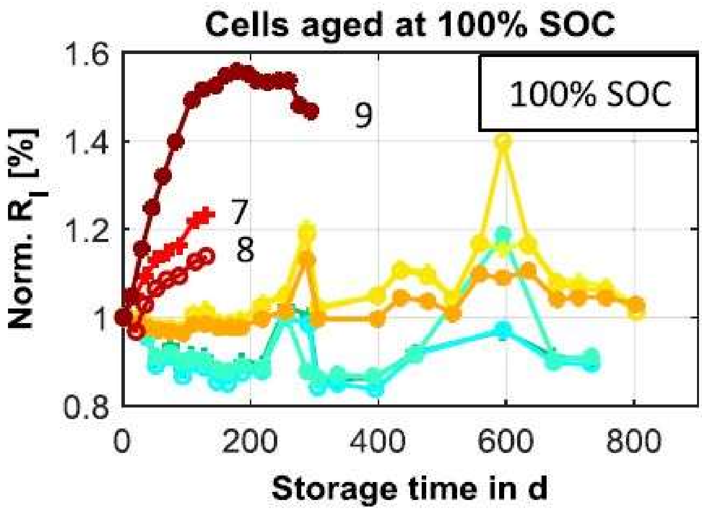

Figure 21: Resistance calendar ageing at 100% SOC and different temperatures. LFP [16]

Similar observations can be made for NMC batteries as illustrated on Figure 22, which however does not present the results at 25°C, the tests were made at 35°C, 50°C and 65°C and 50% of SOC. We can see that after 60 week of storage the resistance increase at 50°C is 50 % higher than the one at 35°C.

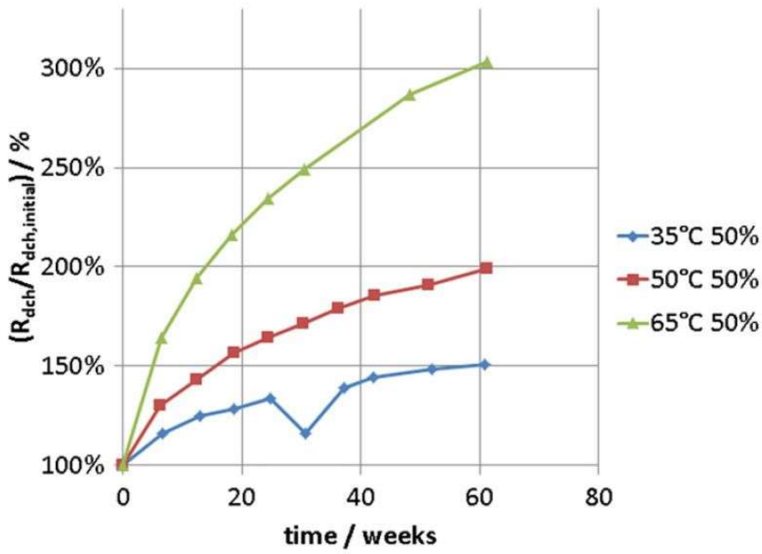

Figure 22: Capacity over storage time at 50% SOC and different temperatures. NMC [13]

7 Effects of combined cycling at temperature above the normal one

The effects described in the previous section are still applicable, but in addition all the other effects described in the other previous sections, like charging and discharging current or depth of discharge, are added, and this result in a combined ageing computation.

7.1 Capacity loss

The temperature at which the battery operates is also an important ageing factor. Figure 23 presents the results of testing at different temperatures (15°C, 45°C and 60°C) for the LFP chemistry, which show that an increase of cycling temperature implies accelerated ageing process in terms of capacity loss. It can be seen that for example cycling at 45°C can reduce the lifetime of the battery of 75 % with respect to cycling at 15°C.

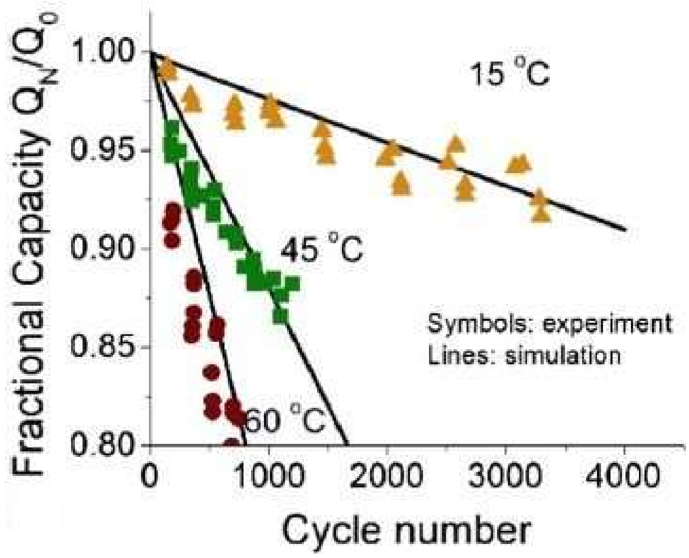

Figure 23: Normalized capacity evolution at different cycling temperatures. LFP [17]

The same observations can be made based on Figure, which is related to the NMC chemistry. It can be seen that an increase of temperature from 25°C to 32°C only can already reduce the lifetime of the battery of 25 %.

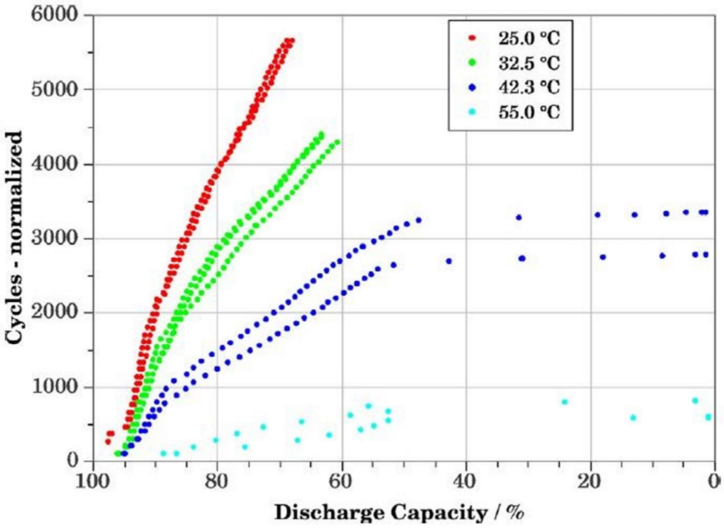

Figure24: Cycling ageing at different temperatures. NMC [15]

The analysis of the figures related to the cycling temperatures allows the construction of a general model, which describes the capacity loss along the cycle lifetime considering a particular operating temperature. This model can then be rescaled to a battery under study according to its specific parameters. It is important to highlight that the results shown in Figure 25 are not available in the literature and have been built by Aurora's Grid.

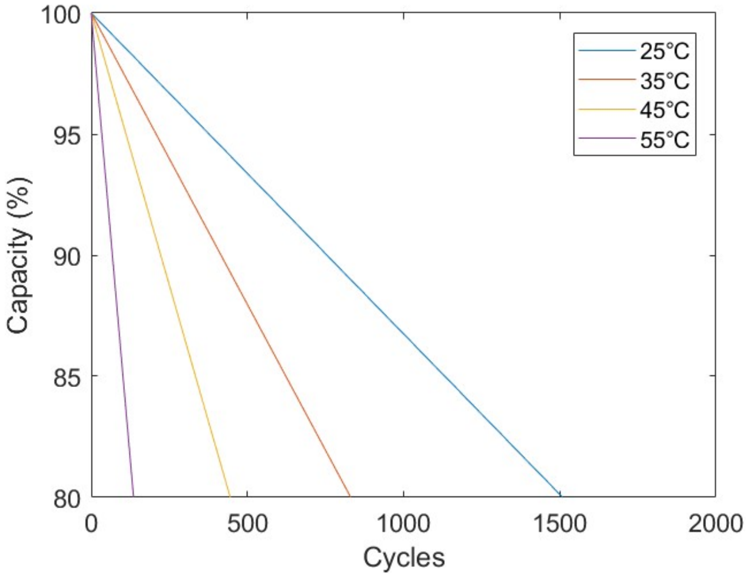

Figure 25: Capacity degradation versus cycle life at different temperatures for a NMC battery [6]

[6] Model developed by Aurora's Grid

7.2 Resistance increase

When it comes to the resistance, the temperature seems to have a smaller impact than the one observed on capacity. Indeed, as can be seen from Figure 26, the increase rate of the internal resistance does not vary significantly between 0°C, 25°C and 40°C. It is only at -18°C, which is an extreme condition, that we observe an important impact.

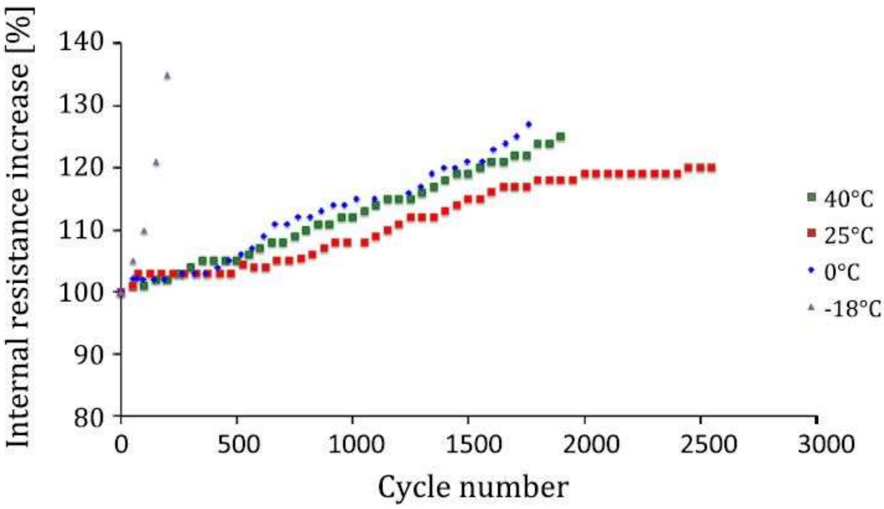

Figure 26: Increase of internal resistance at different temperatures. LFP [8]

8 Effects of abusive high temperature test and evaluation of risk of short-circuit and irreversible performance degradations

Figure 27 represents the energy release diagram of thermal runaway in lithium-ion batteries, it summarizes the chemical kinetics collected from a variety of references. Thermal runaway corresponds to a situation where the temperature in the battery cannot stop to increase due to a chain of exothermic reactions, which leads to vent, fire or even explosion of the cell. The horizontal axis represents the temperature at which a specific decomposition reaction occurs, while the colored "hill-like" regions denotes the chemical kinetics of a specific decomposition reaction with the electrolyte. The following table resumes the abbreviations used in the release diagram [18]:

Table 1: Abbreviations used in Figure 27

Abbreviation	Description
ISC	Internal short circuit
T_{onset}	The onset temperature of the reaction
T_{peak}	The peak temperature of the reaction
T_{end}	The end temperature of the reaction
Q	The maximum heat generation
ΔH	The total energy released during the reaction
SEI-d	The decomposition of the solid electrolyte interface
SEI-regen	The regeneration of the solid electrolyte interface
PE/PP	The melting point of the PE or PP separator
LFP	Decomposition of the LFP cathode with the electrolyte
LTO	Decomposition of the LTO anode with the electrolyte
LCO	Decomposition of the LCO cathode with the electrolyte
NCA	Decomposition of the NCA cathode with the electrolyte
NCM111	Decomposition of the NCM111 cathode with the electrolyte
Gr/C+ele	Decomposition of the graphite/carbon anode with the electrolyte
Ele decomp.	Decomposition of the electrolyte

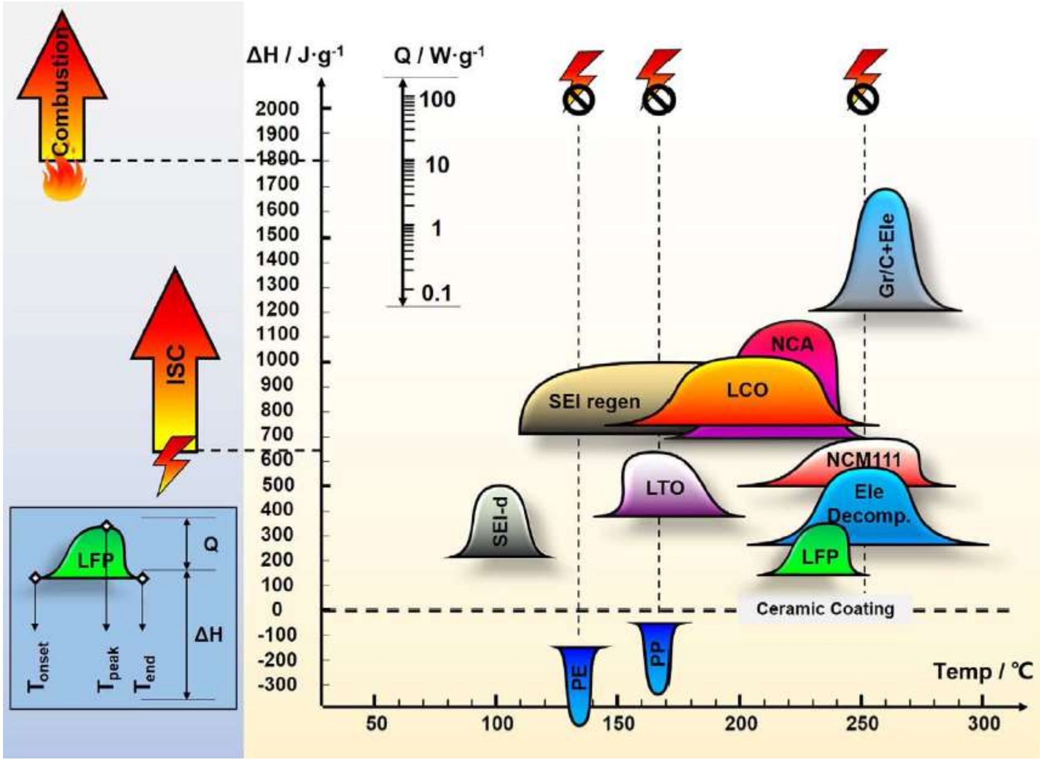

Figure 27: Energy release diagram of lithium ion battery [18]

The first important temperature encountered for every lithium-ion battery technology is 80°C, when the SEI starts to decompose. However, this decomposition is partly counter-balanced by the regeneration of the SEI itself, so the anode decomposition with the electrolyte is postponed and happens only at higher temperatures. The first real problem occurs at the collapse or melting point of the separator which can result in an internal short circuit that consequently leads to the thermal runaway. The problem of the internal short circuit is discussed in the next section. All other reactions happen at much higher temperatures and are beyond the scope of this report.

Figure 28 reports a more detailed chain of reactions as a function of temperature in the specific case of a NMC battery.

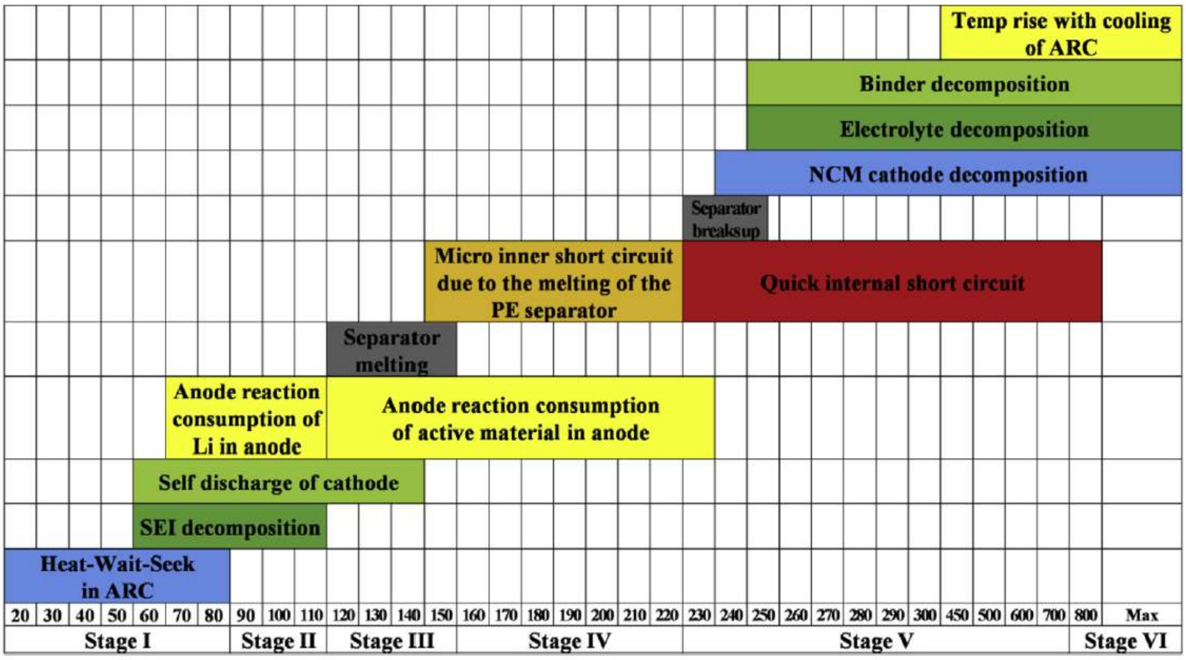

Figure 28: Temperature ranges for different stages of thermal runaway test [19]

Another reference, [20], reports the result of four LFP cells maintained in an oven at 140°C, 150°C, 155°C and 160°C. The first two cells did not reach thermal runaway condition, while the other two do go into thermal runaway. In this case is reported that at about 143°C a large increase in temperature is due to the separator shutdown mechanism which consists in the partially collapse of the separator's pores forming a non-porous insulating film between the two electrodes. However, when the temperature still increases above 150°C the separator meltdown completely allowing the contact between cathode and anode triggering an internal short circuit.

9 Risk of short-circuit in a lithium ion cell

There exist two types of short circuit: internal and external. The external short circuit forms when the two electrodes are connected by low-resistance conductors. This low resistance will cause a flow of high current through the battery that results in fast increase of the temperature.

The ISC is the main cause of thermal runaway and forms when the two electrodes enter in contact due to the failure of the battery separator. This failure can happen in three main situations:

1) Mechanical abuse such as deformation or fracture caused by crush or penetrations;
2) Electrical abuse such overcharge and over-discharge which can damage the separator;
3) Thermal abuse that cause shrinkage and collapsing of the separator resulting in a more sever ISC.

In order to prevent crushes or penetrations in the battery, it is recommended to handle the cells carefully. However, ISC due to mechanical abuse is more likely to happen in the automotive sector, e.g. impact of a car.

When it comes to over-discharging and over-charging the battery, this is a failure due to the malfunctioning of the BMS.

Finally, the triggering of the ISC can happen when the battery is maintained at high temperature. As mentioned before the starting temperature for the ISC is strongly related to the temperature at which the separator melt/collapse. This temperature varies between 130-170°C for polymer separators and can increase to more than 200°C for ceramic separators. This shows the importance of separators in lithium-ion cells [21], [22].

10 Evaluation of lifetime of targeted battery pack with the software Aurora's Grid 1.0

By accounting all the ageing phenomena described above, such as charging current, discharging current, DoD and temperature, this section provides an estimation of lifetime and economic benefit associated with deployment of Li-ions battery storage systems for building equipped with PV rooftop plant. The main goal of installing a Li-ions battery in residential/industrial buildings is to increase the renewable energy self-consumption of the targeted building instead of injecting energy into the grid. The results have been carried out with and without the developed ageing model of Li-ions battery in order to highlight the importance to account for capacity fading.

10.1 Operating conditions

A simulated environment, taking into account real measurement of PV and load consumption (with a sampling time of 15 minutes) has been deployed to emulate the behavior of different sizes of Li-ion BES. The targeted building is located at Neuchatel. The reference household has an annual electricity consumption of roughly 5000 kWh and a PV system of 23 kWp. The simulation period is set to 15 years with the consumption and production profiles being each year equal to the reference data.

The data inputs are the electricity consumption and the PV production profiles, coming from one year of measures of a real household located in Neuchâtel. The energy tariffs and the assumptions were chosen to fit to the 2022 market. More specifically, we do assume an installation battery price of 350 CHF/kWh (the forecasted value for 2022). The energy tariffs are extrapolated from the 2018 Romande Energie tariffs, projected with a 5% increase per year. The retail tariff during peak hours is 0.24 CHF/kWh, while the retail is 0.15 CHF/kWh during off-peak hours and the feed-in tariff is set to be 0.08 CHF/kWh. This last value is really optimistic since, the European trend is to reduce more the feed-in tariff and consequently welcome the installation of BES.

The ageing calculation has been performed thanks to the ageing model previously built by Aurora's Grid.

In summary, the model account for each operating condition of the targeted BES characterized by a specific duration, DoD, current profile and temperature. Then, the model convert this operating condition in an equivalent full cycle at DoD 100% and C-Rate equal to 1C, that is the reference for comparing lifetime of BES.

The economic benefit is calculated by accounting the additional renewable energy self-consumption due to the installation of the BES. Each kWh deployed for the battery has a net benefit equal to the difference between the retail tariff and the feed-in tariff (it is fair to consider the possibility to inject energy into the grid instead of storing it and using later on).

10.2 Simulation results

For the targeted building, the one located at Neuchatel, Figure 29 and 30 illustrate the economic benefit vs the size of the battery and the increase of the energy self-consumption ration vs the size of the BES, respectively.

More specifically, Figure 29 illustrates the evolution of the economic benefit associated with the BES for different cases:

- Without accounting the ageing of the BES, it means constant value of the capacity;
- With the developed ageing model;
- With the ageing model excluding the C-rate effect (the effect of charging and discharging the current with a value different from the nominal one, 1C)
- With the ageing model excluding the middle state of charge (the effect of combined life-calendar and power cycling);
- With a strategy aiming at reducing the ageing of the BES (by limiting C-rate and DoD).

By observing Figure 29, it is possible to make the following observations:

1. The curve not accounting for ageing lead to an economic benefit higher than the one accounting for the whole model. This is due to the fact that the capacity of the BES is constant, and consequently the energy that could be stored and self-consumed is higher as well.
2. The curve not accounting for the middle state of charge effect involves an economic benefit higher than the one accounting for the whole ageing model but lower than the one not accounting for the whole ageing process. This is due to the fact that the capacity associated with has an intermediary value.
3. The most surprising result is that the curve associated with a model excluding the C-rate effect, since it involves an economic benefit lower than the one associated with the whole ageing model. In order to explain this results it is important to remind that in such type of building the power converter coupled with the BES has a nominal power around 0.7-0.8 C.

This means the C-rate is limited by the existing/installed hardware. If we do not account for the C-rate effect it means that we consider each cycle is performed at 1C instead of real value well below the 1-C. Consequently, the ageing process is faster, the capacity reduction and the amount of energy that could be self-consumed as well.

4. The most interesting result is the one associated with an-ageing-aware strategy. In fact, it shows that by correctly limiting the C-rate during charging and discharging phase, the DoD and the middle state of charge is possible to mitigate the ageing phenomena, mitigate the capacity reduction and indirectly increase the energy self-consumption and the overall profitability of the BES (doubling the benefit).

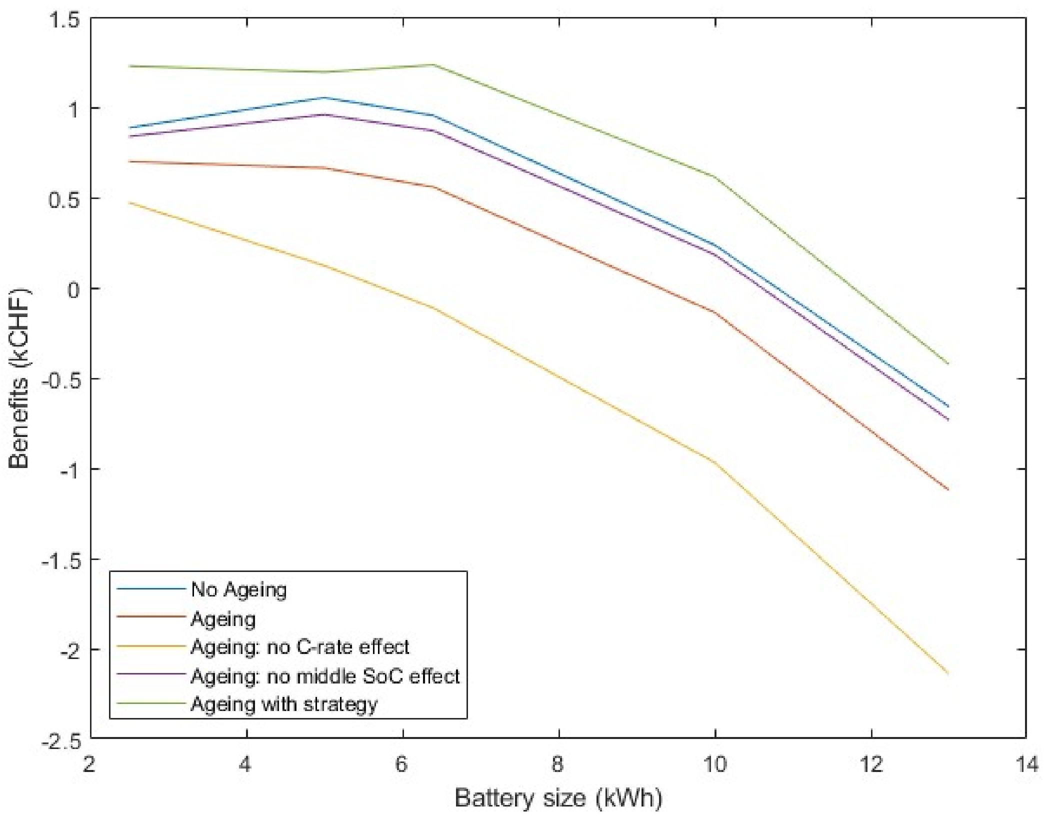

Figure 29: benefit of BES vs its size

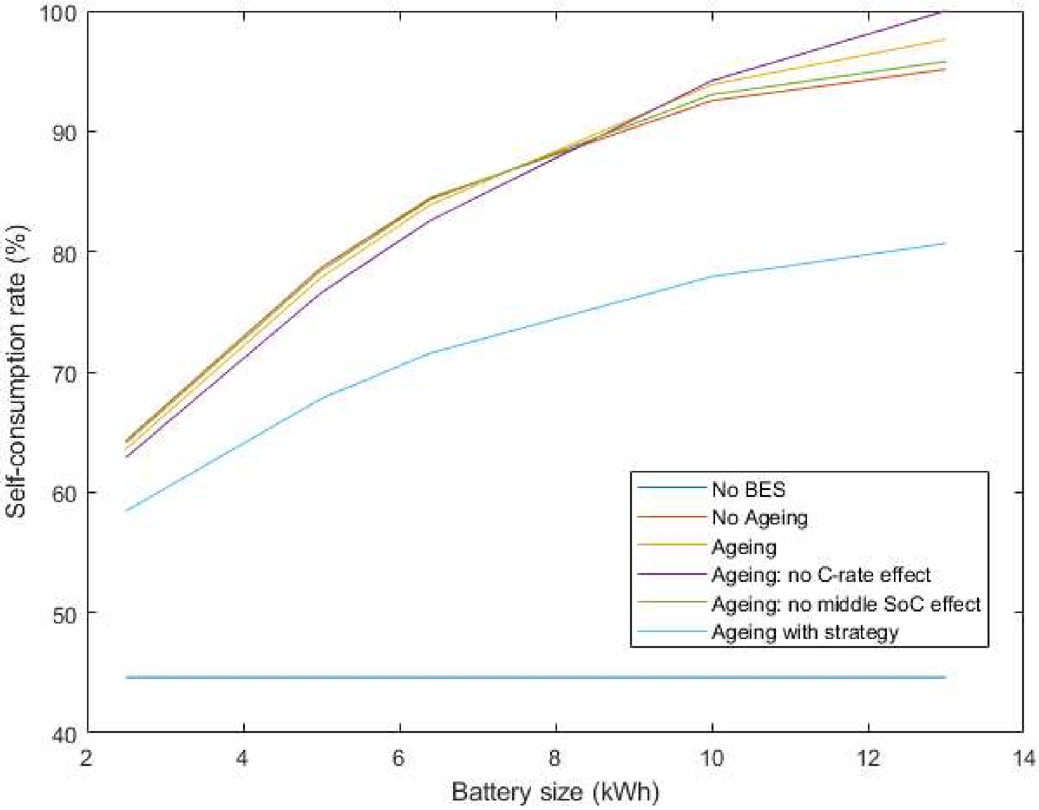

Figure 30: energy self-consumption ratio vs size of the deployed BES.

11 Conclusions and Perspective

This documents shown the importance of the ageing phenomena in Li-ions BES, with a specific focus on C-rate, DoD and temperature effects.

After reviewing the main ageing processes and giving computation of capacity fading and increase of equivalent series resistance for each of the above ageing factors, this document illustrates some simulations results associated with the deployment of BES in buildings.

The presence of BES in a building equipped with a PV plant can be, economically speaking, very interesting. Of course, in order to increase as much as possible its profitability, its lifetime has to be extended by an appropriated ageing-management. The results of this document shown that by managing the ageing of the BES it is possible to double its benefit (compared to a not ageing-aware strategy).

Future works will be focused on the possibility to provide ancillary services to the grid via distributed LI-ions BES located in buildings, in order to increase, much more, the profitability of BES.

Dimitri Torregrossa

Founder and CEO of Aurora's Grid

Lausanne, 27-12-2018

AurorA's Grid

Enabling Ageing-Aware Integration of Battery Storage

Founder and CEO of Aurora's Grid Sàrl *(Enabling Ageing Aware Integration of Energy Storage)*

EPFL Innovation Park, Bâtiment C, 1015 Lausanne

Tel. +41 (0) 787209227

E-mail:dimitri.torregrossa@aurorasgrid.com; dimitri.torregrossa@gmail.com

Website: www.aurorasgrid.com

12 References

[1] P. Keil and A. Jossen, "Charging protocols for lithium-ion batteries and their impact on cycle life-An experimental study with different 18650 high-power cells," *J. Energy Storage*, vol. 6, pp. 125–141, 2016.

[2] P. de Jongh, "Effect of current pulses on lithium intercalation batteries," *Solid State Ionics*, vol. 148, no. 3–4, pp. 259–268, 2002.

[3] X. G. Yang, Y. Leng, G. Zhang, S. Ge, and C. Y. Wang, "Modeling of lithium plating induced aging of lithium-ion batteries: Transition from linear to nonlinear aging," *J. Power Sources*, vol. 360, pp. 28–40, 2017.

[4] C. von Lüders *et al.*, "Lithium plating in lithium-ion batteries investigated by voltage relaxation and in situ neutron diffraction," *J. Power Sources*, vol. 342, pp. 17–23, 2017.

[5] S. F. Schuster *et al.*, "Nonlinear aging characteristics of lithium-ion cells under different operational conditions," vol. 1, pp. 44–53, 2015.

[6] G. Ning, B. Haran, and B. N. Popov, "Capacity fade study of lithium-ion batteries cycled at high discharge rates," *J. Power Sources*, vol. 117, no. 1–2, pp. 160–169, 2003.

[7] J. Vetter *et al.*, "Ageing mechanisms in lithium-ion batteries," *J. Power Sources*, vol. 147, no. 1–2, pp. 269–281, 2005.

[8] N. Omar *et al.*, "Lithium iron phosphate based battery - Assessment of the aging parameters and development of cycle life model," *Appl. Energy*, vol. 113, pp. 1575–1585, 2014.

[9] "LG HD2C 2100mAh constant current test." [Online]. Available: https://www.e-cigarette-forum.com/threads/lg-hd2c-20a-2100mah-18650-bench-test-results-a-25a-2200mah-battery-better-than-the-hd2.735554/.

[10] I. Laresgoiti, S. Käbitz, M. Ecker, and D. U. Sauer, "Modeling mechanical degradation in lithium ion batteries during cycling: Solid electrolyte interphase fracture," *J. Power Sources*, vol. 300, pp. 112–122, 2015.

[11] "PowerTech Systems." [Online]. Available: https://www.powertechsystems.eu/home/tech-corner/lithium-ion-battery-advantages/.

[12] M. Ecker *et al.*, "Calendar and cycle life study of Li(NiMnCo)O2-based 18650 lithium-ion batteries," *J. Power Sources*, vol. 248, pp. 839–851, 2014.

[13] M. Ecker *et al.*, "Development of a lifetime prediction model for lithium-ion batteries based on extended accelerated aging test data," *J. Power Sources*, vol. 215, pp. 248–257, 2012.

[14] A. Eddahech, O. Briat, and J. M. Vinassa, "Performance comparison of four lithium-ion battery technologies under calendar aging," *Energy*, vol. 84, pp. 542–550, 2015.

[15] F. Richter, P. J. S. Vie, S. Kjelstrup, and O. S. Burheim, "Measurements of ageing and thermal conductivity in a secondary NMC-hard carbon Li-ion battery and the impact on internal temperature profiles," *Electrochim. Acta*, vol. 250, pp. 228–237, 2017.

[16] M. Lewerenz *et al.*, "New method evaluating currents keeping the voltage constant for fast and highly resolved measurement of Arrhenius relation and capacity fade," *J. Power Sources*, vol. 353, pp. 144–151, 2017.

[17] J. Li, K. Adewuyi, N. Lotfi, R. G. Landers, and J. Park, "A single particle model with chemical/mechanical degradation physics for lithium ion battery State of Health (SOH) estimation," *Appl. Energy*, vol. 212, no. July 2017, pp. 1178–1190, 2018.

[18] X. Feng, M. Ouyang, X. Liu, L. Lu, Y. Xia, and X. He, "Thermal runaway mechanism of lithium ion battery for electric vehicles: A review," *Energy Storage Mater.*, vol. 10, no. December 2016, pp. 246–267, 2018.

[19] X. Feng *et al.*, “Thermal runaway features of large format prismatic lithium ion battery using extended volume accelerating rate calorimetry,” *J. Power Sources*, vol. 255, pp. 294–301, 2014.
[20] G. Guo, B. Long, B. Cheng, S. Zhou, P. Xu, and B. Cao, “Three-dimensional thermal finite element modeling of lithium-ion battery in thermal abuse application,” *J. Power Sources*, vol. 195, no. 8, pp. 2393–2398, 2010.
[21] E. P. Roth, D. H. Doughty, and D. L. Pile, “Effects of separator breakdown on abuse response of 18650 Li-ion cells,” *J. Power Sources*, vol. 174, no. 2, pp. 579–583, 2007.
[22] C. J. Orendorff, “The Role of Separators in Lithium-Ion Cell Safety,” *Interface Mag.*, vol. 21, no. 2, pp. 61–65, 2012.